Thickness dependence of the magnetic properties of MnAs films on GaAs(001) and GaAs(113)A: Role of a natural array of ferromagnetic stripes

L. Däweritz,[a] L. Wan, B. Jenichen, C. Herrmann, J. Mohanty, A. Trampert, and K. H. Ploog
Paul-Drude-Institut für Festkörperelektronik, Hausvogteiplatz 5-7, D-10117 Berlin, Germany

(Received 15 June 2004; accepted 18 July 2004)

Systematic studies of as-grown MnAs films deposited by molecular-beam epitaxy on GaAs(001) and GaAs(113)A reveal that their magnetic properties and, in particular, their saturation magnetization are determined by the phase separation into stripes of ferromagnetic α-MnAs and paramagnetic β-MnAs. Using a specific saturation magnetization M_S^*, which refers to the actual volume of α-MnAs, the thickness dependence of M_S^* can be described in a universal way. It is due to the variation of the stripe structure and the changing of the intra- and interstripe magnetic interaction. Values well above $\sim$1100 emu/cm^3, obtained for the optimum film thickness at room temperature, are considered as an intrinsic property of a nearly defect-free MnAs in the fully magnetized state. © *2004 American Institute of Physics*. [DOI: 10.1063/1.1790576]

I. INTRODUCTION

The integration of magnetic materials and semiconductor materials has attracted much attention in view of taking advantage of both the highly developed semiconductor technology and the manipulation of spin-polarized carriers.[1,2] MnAs is a very interesting magnetic material with a Curie temperature above room temperature (RT) and a high magnetic moment. For bulk MnAs, RT saturation magnetization values of 600–700 emu/cm^3 have been reported.[3,4] MnAs films have been successfully grown by solid-source molecular-beam epitaxy on various substrates for potential applications;[5,3,6–10] in particular, on GaAs(001), films have been prepared in high quality and their structural and physical properties have been thoroughly studied.[2,3,5–21] Two properties are of crucial importance, the strain-mediated coexistence of α-MnAs and β-MnAs in the epitaxial films [14–19] and a pronounced dependence of their magnetic properties on film thickness.[3,16] Both can be influenced by the growth conditions and the postgrowth annealing process.

Due to the epitaxial strain, the phase transition of the MnAs layers from the paramagnetic orthorhombic β phase (stable in bulk MnAs above $\sim$40 °C) to the ferromagnetic α phase (stable in bulk MnAs below $\sim$40 °C) leads to the coexistence of the two phases over a temperature of nearly 30 °C. This involves a separation into ferromagnetic and paramagnetic stripes running along [0001]. In order to explain the thickness dependence of the magnetic properties and the relatively large scatter in the reported values for the saturation magnetization, one has to consider the complex interplay of phase composition, interface and stripe structure, and magnetic intra- and interstripe interaction.

In this work, we perform a comparative study of MnAs films grown on GaAs(001) and on GaAs(113)A substrates. We restrict ourselves to as-grown films without the additional postgrowth annealing. The GaAs(113)A orientation has been chosen in order to modify intentionally the MnAs/GaAs interface and to investigate whether this affects the magnetic properties of the MnAs films. Although the interfaces are different, the unique stripe pattern of α- and β-MnAs is developed in both cases.[20] By analyzing the geometric and magnetic stripe pattern, we introduce a specific value for the saturation magnetization,[16] which takes into account the real phase composition. We show that in this way, the thickness dependence of the saturation magnetization observed in different laboratories can be well compared. The surprisingly high value above 1100 emu/cm^3 obtained for the saturation magnetization at RT for a defined film thickness is interpreted in terms of an optimum intra- and interstripe magnetic interaction and is considered to be an intrinsic property of MnAs epilayers with drastically reduced defect density.

II. SAMPLE PREPARATION

The MnAs films have been grown on GaAs(113)A and GaAs(001) substrates under the same growth conditions. In order to rule out any uncontrolled influence, two half wafers of (113)A- and (001)-oriented 2-in. substrates were mounted side by side on one sample holder. Thus, they experienced exactly the same growth and cooling procedures. After oxide desorption at 580 °C, a 100-nm-thick buffer layer was grown at 550 °C and an As_4/Ga beam equivalent pressure (BEP) ratio of 20. Then, the substrate temperature was decreased to 230 °C, and the MnAs film was grown at an As_4/Mn BEP ratio of 70 with a growth rate of 20 nm/h. After growth, the substrate temperature was reduced to RT with a rate of 1 °C/min. Thus, the phase transition between β-MnAs and α-MnAs is passed at a very low cooling rate, and the self-organization of the coexisting phases leads to a high uniformity of the stripe structure.[15–20]

It should be noticed that the buffer-layer growth has not been separately optimized for the two different GaAs orientations. In order to investigate the influence of the buffer-layer growth conditions and, consequently, of the surface

[a]Author to whom correspondence should be addressed; electronic mail: daweritz@pdi-berlin.de

morphology on the properties of the MnAs films, similar films have been additionally deposited on GaAs(311)A substrates having buffer layers grown at different temperatures in the range 550–610 °C. The evaluation of the magnetic properties of the MnAs layers deposited on these different buffers revealed no significant differences. This means that any variation of the buffer-layer roughness resulting from the different growth temperatures can be neglected here.

Reflection high-energy electron diffraction (RHEED) was employed to monitor the growth. The observed streaky RHEED pattern indicated that the MnAs growth proceeded on both substrates after coalescence at a thickness of about 1 nm in a quasi two-dimensional mode. The RHEED patterns taken along the orthogonal GaAs$[1\bar{1}0]$ and [110] directions for MnAs/GaAs(001) and the orthogonal GaAs$[1\bar{1}0]$ and $[33\bar{2}]$ directions for MnAs/GaAs(113)A revealed that MnAs grows in the $[\bar{1}100]$ orientation on both substrates. However, using the results of the x-ray measurements, as will be discussed later, in the latter case, there was a slight deviation from the exact $[\bar{1}100]$ orientation. The azimuthal orientations were on GaAs(001): MnAs$[11\bar{2}0]\|$GaAs[110] and MnAs[0001]$\|$GaAs$[\bar{1}10]$; and on GaAs(113)A: MnAs$[11\bar{2}0]\|$GaAs$[1\bar{1}0]$ and MnAs$\sim$[0001]$\|$GaAs$[33\bar{2}]$. On both substrates, the MnAs$(\bar{1}100)$ surface showed a (1×2) reconstruction, i.e., half-order streaks in the RHEED pattern taken along the MnAs[0001] azimuth.

The structural and magnetic properties of the MnAs films on GaAs(001) are known to depend on the film thickness.[3,16] In the present comparative study of the MnAs films on differently oriented GaAs substrates, the film thickness was varied from 50 to 215 nm. To control the film thickness, the Mn flux was calibrated by the RHEED intensity oscillation measurements for MnAs growth on GaAs(001). The actual thicknesses were determined on cross sections of the MnAs/GaAs samples using scanning electron microscopy. Whereas for the MnAs/GaAs(001) samples, these values are close to those expected from a calibration using the RHEED intensity oscillations, there is a tendency for higher values for the MnAs/GaAs(113)A samples grown in the same run.

III. RESULTS AND DISCUSSION

A. Structural properties

1. Phase composition and distribution

As a consequence of the strain energy due to the lattice mismatch and thermal mismatch between MnAs and GaAs in MnAs/GaAs heterostructures, the α and β phases can coexist in the MnAs film at RT.[14,15] The strain arises mainly from the $\beta\rightarrow\alpha$ phase transition during the sample cooling after growth. The lattice parameter along the [0001] direction remains nearly unchanged at this transition. In the (0001) plane, i.e., in the $[11\bar{2}0]$ direction, however, there is an expansion of about 1.2%.[22] The lateral spatial distribution of the two phases in a 180-nm-thick film on GaAs(113)A is imaged in Figs. 1(a) and 1(b) by atomic force microscopy (AFM) and magnetic force microscopy (MFM), respectively.

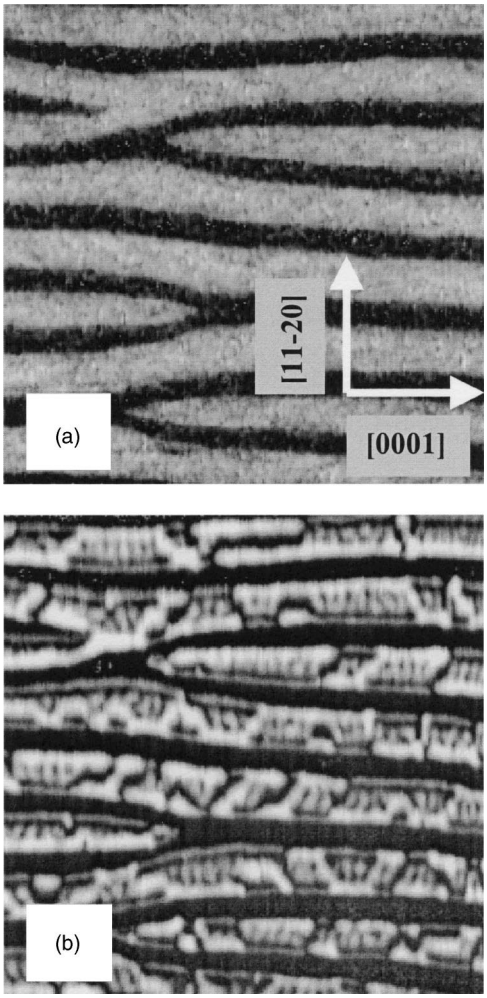

FIG. 1. (a) AFM and (b) MFM images of a 180-nm-thick MnAs film grown on GaAs(113)A. The images show ridges and grooves due to the coexistence of α- and β-MnAs, respectively, and magnetic contrast only in the ferromagnetic α stripes. Image size is 7×7 μm.

As observed in previous studies for MnAs films on GaAs(001),[16,19–21] the AFM image reveals alternating ridges (light stripes) and grooves (dark stripes) running in the [0001] direction. From the magnetic contrast in the MFM image, it follows that the ridges consist of ferromagnetic α -MnAs and the grooves of paramagnetic β-MnAs. The orientation of the stripe pattern is a direct consequence of the anisotropic strain originating at the $\beta\rightarrow\alpha$ phase transition. The surface can be characterized by the periodicity of the stripe pattern P, the width of the ferromagnetic stripes W_{fm}, and the width of the paramagnetic stripes W_{pm}. In Fig. 2, P is plotted as a function of the thickness t of the MnAs film grown on GaAs(001) (squares) and on GaAs(113)A (triangles). We find that P linearly increases with the film thickness for both the GaAs templates. Besides P, W_{fm} and W_{pm} also increase (nearly) linearly with the film thickness. The considerable scatter in the data might be related to the inaccuracy of the data evaluation from the small field of view of the AFM images and/or a variation in the perfection of the MnAs/GaAs interfaces of the used set of samples. There is, however, a reasonable agreement with the results from a very careful measurement [23] of the thickness dependence of P

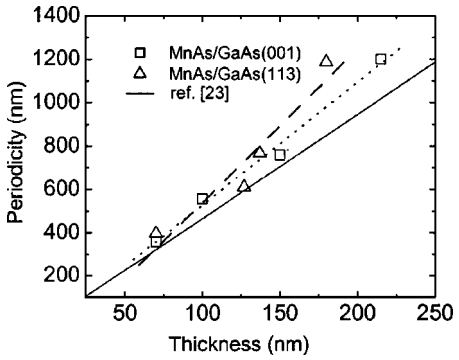

FIG. 2. Dependence of the periodicity of the stripe structure on film thickness for the MnAs films grown on GaAs(001) and on GaAs(113)A represented by squares and triangles, respectively. The dotted and dashed lines are guides to the eye for MnAs/GaAs(001) and MnAs/GaAs(113)A, respectively. The thin full line represents the result of a more accurate LEEM/XMCDPEEM data evaluation from another set of MnAs/GaAs(001) films.

based on the 1arge-fleld images obtained in a combined low-energy electron microscopy (LEEM) and x-ray magnetic circular dichroism photoemission electron microscopy (XMCDPEEM) study [18] of layers grown on very smooth GaAs(001) surfaces prepared by pulsed GaAs deposition. For thicknesses up to 500 nm, P was shown to obey very well the relation $p=1.4t$ (thin solid line in Fig. 2).

As shown, only a fraction of the film consists of ferromagnetic α-MnAs. This is important to understand the magnetic properties of the films. For a quantitave determination of the α-MnAs fraction, we can use the stripe pattern imaged by AFM, MFM, LEEM, XMCDPEEM, or x-ray diffraction. Figure 3 shows a typical ω-2θ scan for a 70-nm thick MnAs film on GaAs(113)A. Two clearly separated peaks for α-MnAs and β-MnAs confirm the phase coexistence at RT. The fraction of α-MnAs obtained from the ratio of the integrated intensities of these peaks is presented in Fig. 4 as a function of the film thickness for the samples grown on GaAs(001) (solid squares) and on GaAs(113)A (solid triangles). These data show that the fraction of α-MnAs is slightly but not significantly higher for the films grown on GaAs(113)A. The same linear dependence on the film thickness is found for both sets of the samples. The values for the α-MnAs fraction estimated from the AFM (MFM) images (open squares and open triangles for films on GaAs(001) and

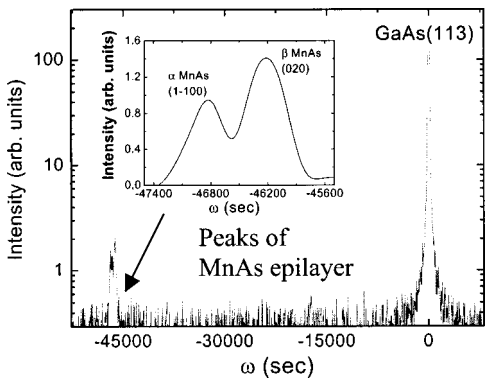

FIG. 3. X-ray diffraction curve (ω-2θ scan) for a MnAs/GaAs(113)A film of 70-nm thickness. The inset shows a smoothed curve in the angular range of interest as used in the data evaluation (cf. Fig. 4).

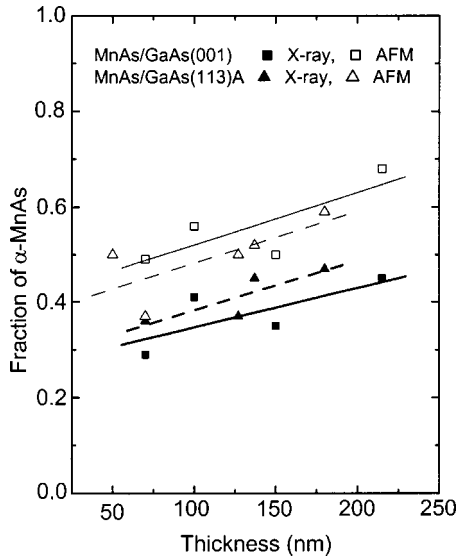

FIG. 4. Thickness dependence of the α-MnAs fraction in films grown on GaAs(001) and GaAs(113)A deduced from the x-ray data (full symbols) and AFM data (open symbols). The lines are guides to the eye.

GaAs(113)A, respectively) are apparently systematically higher than those determined by x-ray diffraction. An overestimation is to be expected because of the irregularities in the stripe pattern,[20] as seen also in Fig. 1, are neglected.

2. Microstructure

Besides the strain-mediated phase coexistence, other strain relaxation mechanisms in MnAs/GaAs heterostructures are also relevant. Here, we are interested in the differences of these mechanisms for the two types of sample orientations, which lead to the different microstructures of the films. Considering the interface configurations of MnAs/GaAs(113)A and MnAs/GaAs(001) along MnAs$[11\bar{2}0]$, we find exactly the same crystal directions in both the epilayers and the substrates if we do not distinguish between the $[110]$ and $[1\bar{1}0]$ directions of GaAs(001). The strain relaxation mechanism for both types of samples along this direction should hence be the same, and therefore, the characteristic stripe pattern discussed before is observed in both cases. The strain relaxation mechanism has been studied by high-resolution transmission electron microscopy (HRTEM) for the MnAs/GaAs(001) heterostructure.[12] The misfit strain along the MnAs$[11\bar{2}0]$ direction is relieved by the formation of regularly arranged misfit dislocations, which is thus expected for MnAs/GaAs(113)A, too. Along the MnAs$[0001]$ direction, the relaxed interface structure for MnAs/GaAs(001) is composed of commensurate domains having a perfect coincidence arrangement, which are separated by extended secondary dislocations.[12]

For MnAs/GaAs(113)A, however, the interface configuration along the MnAs$[0001]$ direction should be different as the c axis is tilted out of plane.[24] Figure 5 shows a cross-sectional HRTEM image of the MnAs/GaAs(113)A heterostructure in the MnAs$[11\bar{2}0]\|$GaAs$[1\bar{1}0]$ projection. Because of the different interference patterns on both sides of the heterostructure, the interface can be determined accurately.

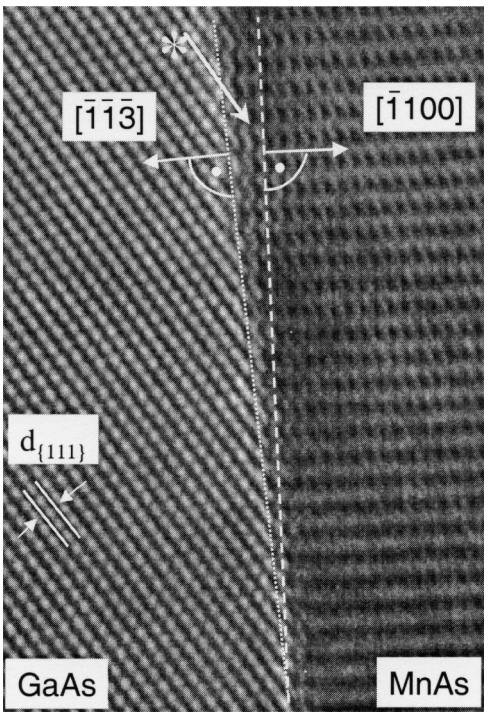

FIG. 5. Cross-sectional HRTEM image of the MnAs/GaAs(113)A interface in MnAs[11$\bar{2}$0]‖GaAs[1$\bar{1}$0] projection. The dotted and dashed lines mark the interface and the trace of a MnAs(1$\bar{1}$00) plane, respectively. The MnAs(1$\bar{1}$00) growth direction is tilted with respect to the {113} orientation of the substrate. The alignment of the MnAs(1$\bar{1}$00) lattice planes with the GaAs{111} lattice planes is indicated by the arrow marked by a star.

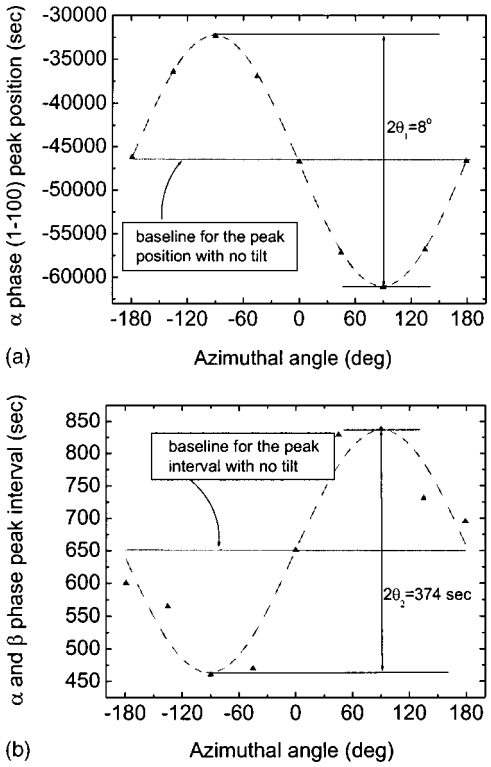

FIG. 6. MnAs epilayer tilt in the MnAs/GaAs(113)A films as observed by the x-ray measurements. (a) Tilt angle as a sine function of the azimuthal angle indicating that the MnAs(1$\bar{1}$00) plane is not parallel to the substrate surface. The zero-degree azimuth is set as the x-ray incident plane parallel to MnAs[11$\bar{2}$0]. (b) Measurement of the tilt angle (out of plane) between α- and β-MnAs stripes. The [000$\bar{1}$] direction is tilted out of plane from the GaAs[33$\bar{2}$] axis around the [11$\bar{2}$0] axis by 4°, while the [11$\bar{2}$0] axis keeps in plane. The out-of-plane tilt angle between the stripes of α- and β -MnAs is 0.05.

The interface, which appears atomically abrupt, is highlighted by the thin dotted line, whereas the dashed line is the trace of the MnAs(1$\bar{1}$00) plane. It is obvious that the GaAs[1$\bar{1}$3] and MnAs[1$\bar{1}$00] directions do not coincide; the MnAs[1$\bar{1}$00] direction is a few degrees tilted from GaAs[1$\bar{1}$3]. We measured the accurate epitaxial relationship of the MnAs/GaAs(113)A films using high-resolution x-ray diffraction (HRXRD). The symmetrical diffraction peaks from the substrate are used as references, i.e., GaAs(113) and GaAs(004) for the different substrate orientations. The samples were rotated azimuthally around the growth direction (surface normal), and for several azimuths, radial (i.e., $\omega-2\theta$) scans were performed. For each scan, the separation between MnAs(1$\bar{1}$00) and the corresponding reference peak was obtained. If the (1$\bar{1}$00)MnAs planes were parallel to the growth surface, the separation of the reference peak would not change in dependence of the azimuthal angle. This was indeed observed for MnAs/GaAs(001) in agreement with the RHEED results. During the azimuthal rotation of the MnAs/GaAs(113)A samples, this peak separation follows a sine function, as shown in Fig. 6(a). This indicates that the (1$\bar{1}$00)MnAs planes are tilted,[25] and the observed tilt angle is 4° around the MnAs[11$\bar{2}$0] axis. The MnAs[11$\bar{2}$0] direction remains parallel to GaAs[1$\bar{1}$0]. A minor tilt angle between the α- and β-MnAs domains of 0.05° was derived from the data of Fig. 6(b). In contrast, in the MnAs/GaAs(001) samples, the orientations of both phases are parallel.

Along the perpendicular MnAs[0001] in-plane direction, i.e., along the *c* axis, the interface configurations are different as the *c* axis is tilted out of the interface plane in the MnAs/GaAs(113)A layer, whereas in the MnAs/GaAs(001) 1ayer, the *c* axis remains in the interface plane. The corresponding net plane distances are also different. This gives evidence for different strain relaxation mechanisms along this direction.

The observed tilt of the *c* axis in the MnAs/GaAs(113)A samples can be understood in terms of an energy-minimizing lattice mismatch accommodation process. Considering the [0001] direction, in the case of the MnAs/GaAs(001) layer, four MnAs(0002) atomic planes match six GaAs(2$\bar{2}$0) planes, as observed by the HRTEM.[12] In this way, the effective lattice mismatch between the layer and the substrate is reduced from 30% to 5% by the formation of a coincidence lattice. In the case of the MnAs/GaAs(113)A samples, however, the HRTEM and HRXRD results reveal an alternative mechanism for the mismatch accommodation process. The 4° tilt from the singular MnAs[1$\bar{1}$00] growth direction in the case of the MnAs/GaAs(113)A films promotes the generation of a coherent interface by improving the alignment of the {1$\bar{1}$00} lattice planes in MnAs with the {111} lattice planes in GaAs, as highlighted in Fig. 5 by the arrow marked by a star. Both sets of lattice planes play an important role as

step edges during growth. Here, it is important to notice that there are two different contributions to the morphology of the MnAs films: (i) the periodic undulations due to the groove-ridge structure described previously and (ii) the step morphology.[16,19] The former is caused by the elastic distortion of the film during cooling due to the presence of α- and β-phase MnAs in the film; the latter is formed during growth. As shown for MnAs/GaAs(001) by using scanning-tunneling electron microscopy, one system of monolayer growth steps is running along MnAs$[11\bar{2}0]$.[19] It is obvious that these steps will also exist on the MnAs/GaAs(113)A films. There, the edges of these growth steps could play an important role in the experimentally observed alignment of the $\{\bar{1}101\}$ lattice planes in MnAs with the {111} lattice planes in GaAs.

B. Magnetic properties

The magnetic properties of the MnAs films were determined by using superconducting quantum interference device (SQUID) magnetometry. All measurements were performed with the external field applied along MnAs$[1\bar{1}20]$, which is the easy axis of magnetization. The hysteresis loops measured at RT for the MnAs/GaAs(113)A films of different thicknesses are presented in Fig. 7(a). An almost square loop is observed for the 70-nm-thick film. With the increasing film thickness, the loop inclines gradually and becomes more complex. Whereas the coercive field decreases, a higher external field is needed for the magnetization of the thicker films. The main reason for this changing shape of the hysteresis loop is assumed to be the attenuation of the coupling strength between the ferromagnetic α-MnAs stripes due to their wider separation in thicker films. The characteristic change in the shape of the hysteresis loop occurs at a separation W_{pm} in the order of 200 nm. The ferromagnetic coupling between the neighboring stripes then becomes weaker. This can be seen from the array of magnetic domains in the MFM image taken from a 180-nm-thick MnAs/GaAs(113)A film and shown in Fig. 1(b). The magnetic moments within a single domain lie either all along the MnAs$[\bar{1}\bar{1}20]$ or all along the MnAs$[1\bar{1}20]$ direction. The domains are imaged as comblike structures, which show up in these two opposite orientations within an individual stripe of α-MnAs. A detailed description of the domain structure has been given e1sewhere.[11,21] As a consequence of the reduced intra- and interstripe coupling, a higher external field is needed for the magnetic saturation. The same tendency for the thickness dependence of the loop shape is found also for the MnAs/GaAs(001) films, as can be seen from Fig. 7(b). For a 40-nm-thick film, a direct insight into the ferromagnetic coupling of the stripes has been obtained in a LEEM/XMCDPEEM study.[18] As schematically shown in Fig. 8(a), the XMCDPEEM image of the film in the $\alpha \rightarrow \beta$ transition stage, upon heating from below 273 K, reveals ferromagnetic domains, which are strongly elongated in the [0001] direction. In neighboring domain, the magnetic moments are oriented opposite to each other. The paramagnetic stripes perpendicular to the easy axis break the domains up into

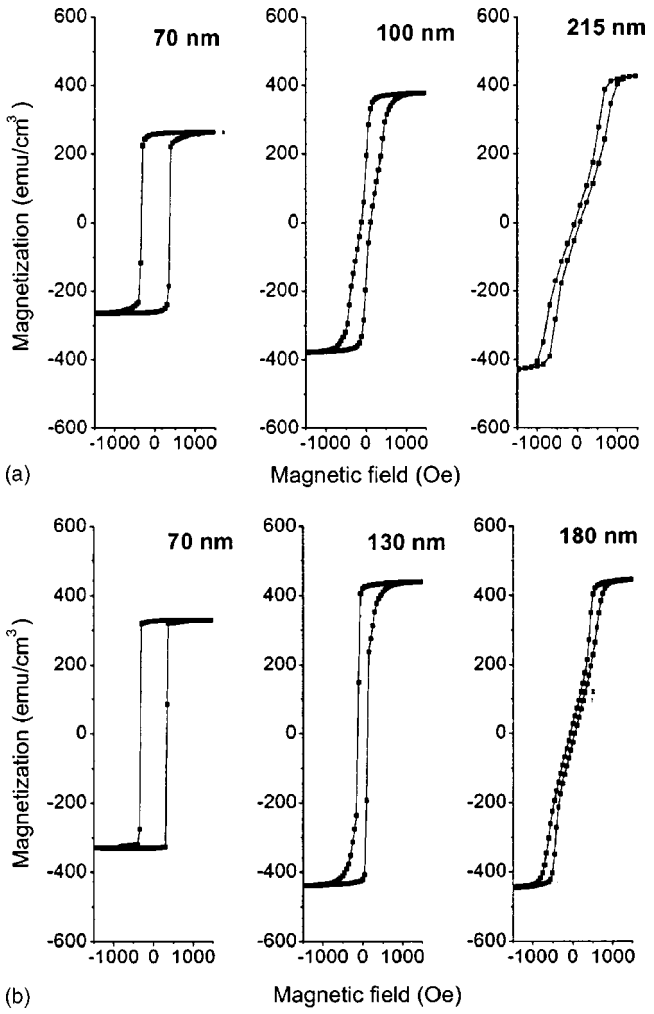

FIG. 7. Hysteresis loops obtained by SQUID measurements at room temperature with the magnetic field applied along the easy axis of magnetization for the films grown on (a) GaAs(001) and on (b) GaAs(113)A. The thickness of the films is indicated.

narrow stripes, which are still well correlated. In a MnAs film cooled from the completely paramagnetic state to RT, there is yet mainly ferromagnetic coupling between the neighboring ferromagnetic stripes. But many oppositely magnetized regions occur, too, as sketched in Fig. 8(b). When the ferromagnetic stripes become wider in thicker films, then they become subdivided into subdomains not only along but also across the stripe. This will be discussed else-

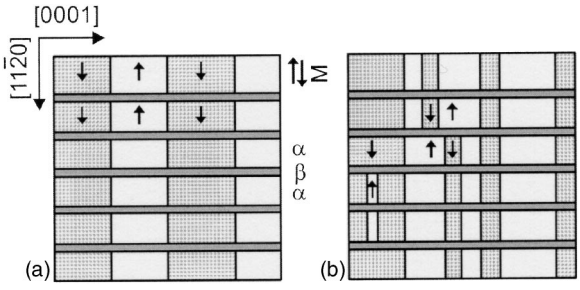

FIG. 8. Schematic representation of the array of magnetic domains in the coexistence range of the α and β phase of a thin MnAs film (a) as expected upon heating from the fully magnetized state and (b) as observed [18] upon the cooling from the completely paramagnetic state to room temperature.

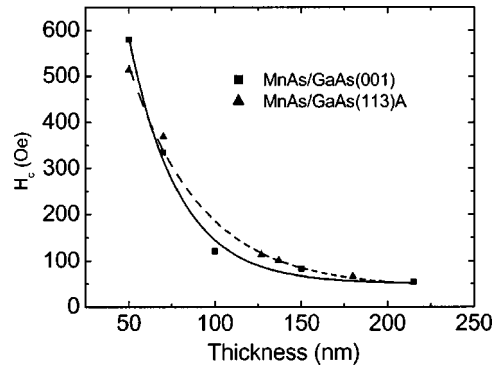

FIG. 9. Coercive field H_c as a function of film thickness obtained from the hysteresis loops measured for the MnAs/GaAs(001) and the GaAs(113)A films at RT.

where in detail.[23] Thus, the saturation magnetization depends on the ferromagnetic intrastripe and interstripe interactions. The RT coercive field H_C was derived from the hysteresis loops. Its thickness dependence is comparable for both types of the MnAs films, as can be seen in Fig. 9.

When evaluating the magnetic properties of the films, one has to take into account that they only partly consist of ferromagnetic α-MnAs. Therefore, a specific saturation magnetization M_S^* has been introduced, which refers to the volume of α-MnAs determined by x-ray diffraction.[16] Here, we will additionally use a specific saturation magnetization M_S^{**}, which is based on a volume evaluation of α-MnAs from the AFM data. Figure 10(a) shows the as-measured data for the thickness dependence of the saturation magnetization M_S^*. The squares and triangles refer to the films grown on GaAs(001) and GaAs(113)A, respectively. For the MnAs/GaAs(001) films, we observe an increase of M_S up to a film thickness of about 70–100 nm. Also shown is a replot of the data for MnAs/GaAs(001) taken from the early work of Tanaka *et al.*[3] It reveals a similar behavior as the present data, although M_S shows a peak already at 50 nm and then decreases. Most likely, this can be attributed to a higher content of α-MnAs in the samples of Ref. 3, whereas for the preparation conditions of our samples (nonoptimized template, no postgrowth annealing), it is only about 50% and varies considerably. More instructive are the values M_S^* and M_s^{**} [Figs. 10(b) and 10(c) respectively], which refer to the volume of α-MnAs. The M_S^* values for MnAs/GaAs(001) rapidly increase from about 500 emu/cm^3 at 50 nm film thickness to a value as high as ~1100 emu/cm^3 at 70 nm and then gradually decrease to ~900 emu/cm^3 at 215 nm. The general behavior of the thickness dependence of M_s^* is now very similar to that of M_s found by Tanaka *et al.*[3] However, the curve is shifted to considerably higher values, peaking at ~1100 emu/cm^3, which is close to the saturation magnetization of ~1200 emu/cm^3 reported for MnAs/GaAs(001) at 10 K.[13] This considerably exceeds the room-temperature saturation values of 600–700 emu/cm^3 reported for bulk MnAs.[3,4] Even the value of ~790 emu/cm^3 at a 100-nm film thickness [Fig. 10(c)], which is expected to underestimate the real value, is clearly higher. This shows that the peak value of the saturation magnetization for a defined film thickness requires a material with an optimum intra- and interstripe magnetic coupling.

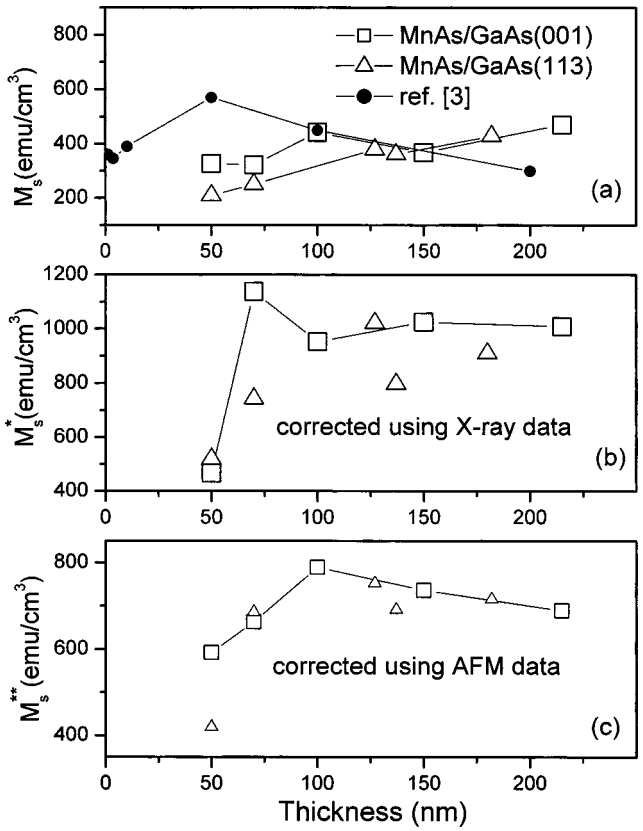

FIG. 10. Thickness dependence of the saturation magnetization at RT for the MnAs/GaAs(001) and MnAs(113)A films. (a) As-measured saturation magnetization M_S, (b) the corrected values of M_s^* based on the x-ray data, and (c) M_S^{**} based on the AFM data.

The data presented in Figs. 10(a)–10(c) reveal that the MnAs/GaAs(113)A films show a similar behavior of the thickness-dependent magnetic properties as the MnAs/GaAs(001) films. A slight but not significant tendency to lower magnetization values and stronger scatter of the data is a hint that the formation of the coupled ferromagnetic MnAs stripes is less perfect on GaAs(113)A than on GaAs(001), as a consequence of the differences in the interface structure

IV. CONCLUSIONS

In summary, a detailed analysis of the structural and magnetic properties of as-grown MnAs films deposited on (001)- and (113)A-oriented GaAs substrates has been presented. We have shown that a unique pattern of ferromagnetic and paramagnetic stripes due to phase separation into α- and β-MnAs is formed independently whether the films are deposited on GaAs(001) or GaAs(113)A and even though the interface structure is different for the two substrate orientations. By introducing a specific value for the saturation magnetization, which takes into account the real phase composition, the thickness dependence of the saturation magnetization observed in different laboratories can be well compared. The stripe pattern, representing an array of micromagnets, changes in a characteristic manner with the

film thickness. At a certain thickness (around 70 nm in the present study), the ferromagnetic intrastripe and interstripe interactions become optimum, leading to a very high stripe specific saturation magnetization even at RT. A value well above 1000 emu/cm^3 is considered to be an intrinsic property of a (nearly) defect-free α-MnAs in the fully magnetized state.

ACKNOWLEDGMENTS

The authors thank T. Hesjedal for supporting the AFM/MFM measurements. This work has been partly supported by the Bundesministerium für Forschung und Technologie.

[1]G. A. Prinz, Science **250**, 1092 (1990).
[2]M. Tanaka, Semicond. Sci. Technol. **17**, 327 (2002).
[3]M. Tanaka, J. P. Harbison, M. C. Park, Y. S. Park, T. Shin, and G. M. Rothberg, J. Appl. Phys. **76**, 6278 (1994).
[4]N. Menyuk, J. A. Kafalas, K. Dwight, and J. B. Goodenough, Phys. Rev. **177**, 942 (1969).
[5]M. Tanaka, J. P. Harbison, M. C. Park, Y. S. Park, T. Shin, and G. M. Rothberg, Appl. Phys. Lett. **65**, 1964 (1994).
[6]F. Schippan, A. Trampert, L. Däweritz, and K. H. Ploog, J. Vac. Sci. Technol. B **17**, 1716 (1999).
[7]S. Sugahara and M. Tanaka, J. Appl. Phys. **89**, 6677 (2001).
[8]M. Kästner, L. Däweritz, and K. H. Ploog, Surf. Sci. **511**, 323 (2002).
[9]K. Akeura, M. Tanaka, M. Ueki, and T. Nishinaga, Appl. Phys. Lett. **67**, 3349 (1995).
[10]K. Akeura, M. Tanaka, T. Nishinaga, and J. DeBoeck, J. Appl. Phys. **79**, 4957 (1996).
[11]F. Schippan, G. Behme, L. Däweritz, K. H. Ploog, B. Dennis, K.-U. Neumann, and K. R. A. Ziebeck, J. Appl. Phys. **88**, 2766 (2000).
[12]A. Trampert, F. Schippan, L. Däweritz, and K. H. Ploog, Appl. Phys. Lett. **78**, 2461 (2001).
[13]J. J. Berry, S. J. Potashnik, S. H. Chun, K. C. Ku, P. Schiffer, and N. Samarth, Phys. Rev. B **64**, 052408 (2001).
[14]V. M. Kaganer, B. Jenichen, F. Schippan, W. Braun, L. Däweritz, and K. H. Ploog, Phys. Rev. Lett. **85**, 341 (2000).
[15]V. M. Kaganer, B. Jenichen, F. Schippan, W. Braun, L. Däweritz, and K. H. Ploog, Phys. Rev. B **66**, 045305 (2002).
[16]L. Däweritz *et al.*, Proceedings of the 28th International Symposium on Compound Semiconductors ,edited by Y. Arakawa, Y. Hirayama, K. Kishnino, and H. Yamaguchi, IOP Conf.ser.170 p. 269 (2002).
[17]T. Plake, M. Ramsteiner, V. M. Kaganer, B. Jenichen, M. Kästner, L. Däweritz, and K. H. Ploog, Appl. Phys. Lett. **80**, 2523 (2002).
[18]E. Bauer, S. Cherifi, L. Däweritz, M. Kaestner, S. Heun, and A. Locatelli, J. Vac. Sci. Technol. B **20** 2539 (2002).
[19]M. Kästner, C. Herrmann, L. Däwertiz, and K. H. Ploog, J. Appl. Phys. **92**, 5711 (2002).
[20]L. Däwertiz, M. Kästner, T. Hesjedal, T. Plake, B. Jenichen, and K. H. Ploog, J. Cryst. Growth **251**, 297 (2003).
[21]R. Engel-Herbert, J. Mohanty, A. Ney, T. Hesjedal, L. Däweritz, and K. H. Ploog, Appl. Phys. Lett. **84**, 1132 (2004).
[22]B. T. Willis, and H. P. Rooksby, Proc. Phys. Soc. London, Sect. B **67**, 290 (1954).
[23]E. Bauer *et al.* (unpublished).
[24]A. Trampert., Physica E (Amsterdam) **13**, 1119 (2002).
[25]A. Pesekt, K. Hingerl, F. Riesz, and K. Lischka, Semicond. Sci. Technol. **6**, 705 (1991).